Oncogene (2008) 27, 3912–3922

www.nature.com/onc

ORIGINAL ARTICLE

Oncogenic role of DDX3 in breast cancer biogenesis

M Botlagunta[1], F Vesuna[1], Y Mironchik[1], A Raman[2], A Lisok[1], P Winnard Jr[1], S Mukadam[1], P Van Diest[3], JH Chen[4], P Farabaugh[2], AH Patel[5] and V Raman[1,6]

[1]*Department of Radiology and Radiological Sciences, Johns Hopkins University School of Medicine, Baltimore, MD, USA;* [2]*Department of Biology, University of Maryland, Baltimore, MD, USA;* [3]*Department of Pathology, University Medical Center Utrecht, Utrecht, The Netherlands;* [4]*Department of Life Science, Tzu Chi University, Hualien, Taiwan;* [5]*Arvind Patel-Institute of Virology, Glasgow-G11, UK and* [6]*Department of Oncology, Johns Hopkins University School of Medicine, Baltimore, MD, USA*

Benzo[a]pyrene diol epoxide (BPDE), the active metabolite of benzo[a]pyrene present in tobacco smoke, is a major cancer-causing compound. To evaluate the effects of BPDE on human breast epithelial cells, we exposed an immortalized human breast cell line, MCF 10A, to BPDE and characterized the gene expression pattern. Of the differential genes expressed, we found consistent activation of DDX3, a member of the DEAD box RNA helicase family. Overexpression of DDX3 in MCF 10A cells induced an epithelial-mesenchymal-like transformation, exhibited increased motility and invasive properties, and formed colonies in soft-agar assays. Besides the altered phenotype, MCF 10A-DDX3 cells repressed E-cadherin expression as demonstrated by both immunoblots and by E-cadherin promoter-reporter assays. In addition, an *in vivo* association of DDX3 and the E-cadherin promoter was demonstrated by chromatin immunoprecipitation assays. Collectively, these results demonstrate that the activation of DDX3 by BPDE, can promote growth, proliferation and neoplastic transformation of breast epithelial cells.
Oncogene (2008) **27,** 3912–3922; doi:10.1038/onc.2008.33; published online 11 February 2008

Keywords: DDX3; breast cancer; BPDE

Introduction

Breast cancer is the second leading cause of cancer-related deaths in American women (Parkin and Muir, 1992; Sasco, 2001). The etiology of breast cancer can be associated with a number of factors such as nulliparity, age, hormonal factors, alcohol intake and so on (Norsa'adah *et al*., 2005; Boffetta *et al*., 2006; Yager and Davidson, 2006). However, many of these factors account for less than one-half of all sporadic cases (Phillips *et al*., 1991). Thus, it is likely that environmental factors are also involved in the development of breast cancer. A member of a class of environmental pollutants (polycyclic aromatic hydrocarbons) that may contribute to human breast cancer is benzo(a)pyrene (BaP), a major constituent of tobacco smoke (Reynolds *et al*., 2004). The highly reactive epoxy metabolite of BaP, benzo[a]pyrene diol epoxide (BPDE), can form stable DNA adducts, for example, within *Ha-ras* oncogene, and initiate carcinogenesis as shown in human fibroblasts and CHO cell lines (Krolewski *et al*., 1988; Yang *et al*., 1992). Moreover, there is emerging evidence that indicates that human mammary epithelium may be susceptible to carcinogenic transformation upon exposure to BPDE (Mei *et al*., 2003). For instance, human mammary epithelial cells and breast cancer cell lines, exposed to BPDE, exhibited altered cell cycle progression, decreased BRCA-1 expression and an increased spectrum of p53 mutations (Jeffy *et al*., 2002; Pfeifer *et al*., 2002; Wang *et al*., 2003; Burdick *et al*., 2006). It has also been shown that treating MCF 10A cells with 1 μM of B[a]P for 48 hours is sufficient to cause chromosomal aberrations and induce anchorage-independent growth (Caruso *et al*., 2001). This indicates that carcinogens present in tobacco smoke may be a contributing factor in the etiology of breast cancers. Thus, we have initiated studies aimed at characterizing cellular components and pathways, at the molecular level, that are altered during an exposure to BPDE.

In our efforts to understand better the transforming abilities of BPDE, within the context of human breast epithelial cells, we have identified a member of the DEAD box RNA helicase family, DDX3, which is upregulated after exposing immortalized non-tumorigenic breast epithelial cells, MCF 10A, to BPDE. DEAD box RNA helicases have been shown to function in RNA metabolism including translation, ribosome biogenesis, pre-mRNA splicing and nucleo-cytoplasmic RNA transport (Cordin *et al*., 2006; Linder, 2006). Besides their role in RNA biogenesis there is now evidence to indicate that DEAD box RNA helicases can participate in the progression of cancer (Abdelhaleem, 2005). For example, human DDX5 has been shown to be overexpressed at the protein level in colorectal tumors as well as in the hepatic tumor cell lines, HT-29 and HCT116, which have undergone an

Correspondence: Dr V Raman, Radiology, Johns Hopkins University School of Medicine, 720 Rutlands Avenue, 340 Traylor Bldg, Baltimore, MD 21205, USA.
E-mail: vraman2@jhmi.edu
Received 14 September 2007; revised 3 January 2008; accepted 4 January 2008; published online 11 February 2008

epithelial-mesenchymal transition (Yang *et al*., 2005, 2006). In addition, DDX5 has been shown to upregulate the expression of cyclin D1 along with c-myc genes, which promoted cell proliferation in a series of mammalian cell lines (Yang *et al*., 2007). Along these lines, the activity of oncoprotein EWS-FLI1 has been shown to be enhanced by RNA helicase H in the Ewing's sarcoma family of tumors (Toretsky *et al*., 2006). The X-linked DEAD box RNA helicase, DDX3 has been shown to be upregulated in hepatocellular carcinoma tissues and through its interaction with hepatitis C virus core protein, may be a contributing factor to hepatitis C virus-mediated carcinogenic processes (Owsianka and Patel, 1999; Huang *et al*., 2004). However, in another study, DDX3 in hepatocellular carcinoma cell lines was shown to transcriptionally upregulate the tumor suppressor molecule, p21, thus decreasing cell proliferation (Chang *et al*., 2006; Chao *et al*., 2006). Also, DDX3 has been shown to be inactivated in HeLa cells during mitosis via the phosphorylation of Threonine 204 by the cyclinB/cdc2 complex (Sekiguchi *et al*., 2007). Thus, the role of DDX3 in cancer biogenesis appears to be divergent and tumor type-dependent.

In this report, we show that the expression of DDX3 is enhanced in the breast epithelial cell line MCF 10A upon exposure to BPDE. Also, stable overexpression of DDX3 in MCF 10A cells induces an epithelial-mesenchymal-like transition and promotes aggressive properties such as increased motility and invasion as well as the ability to form colonies in soft agar, which are the characteristic features of cellular transformation. In addition, our data also demonstrate that DDX3 expression downregulates the expression of the cell adhesion molecule E-cadherin, resulting in the translocation of β-catenin into the nucleus. Taken together, we show that overexpression of DDX3 in mammary epithelium can promote breast tumorigenesis.

Results

Effect of BPDE on the growth and viability of MCF 10A cells

To identify potential candidate genes induced by BPDE in MCF 10A cells, the optimal concentration of BPDE and its incubation time with cells were determined. The growth ratio and percentage of viable cells were estimated at 3, 10 and 24 h following exposure to increasing concentrations of BPDE (0.5, 1, 1.5, 2, 2.5 and 3 μM). Figure 1a (left panel) indicates that MCF 10A cells exposed to concentrations of BPDE above 0.5 μM showed a continual decline in growth during the 24 h period, with respect to control cultures. However, BPDE concentrations at or below 0.5 μM had little or no affect on cell growth during the 3- and 10-h incubation periods. On the contrary, when the cultures were exposed to 1.5 μM BPDE, cell growth was reduced by approximately 55% during the 10-h period. As shown in Figure 1a (right panel), cell viability remained unaffected at all BPDE concentrations during the initial 3 h. However, very few viable cells remained when cultures were exposed to 1.0 μM BPDE for 24 h. On the basis of this data, MCF 10A cells were incubated with 0.5 μM of BPDE for 3 and 10 h, and RNA was extracted at each time point. Following Affymetrix microarray data analyses, DDX3 was one of the genes that was found to be upregulated approximately fourfold in MCF 10A cells treated with BPDE.

BPDE induces DDX3 expression in mammary epithelial cells

Having identified that DDX3 gene expression is induced by BPDE, we proceeded to test the finding at the protein level in MCF 10A and MCF 12A cell lines. Following incubation in 0.5 μM BPDE for 1 h, the cells were washed and replenished with complete medium and incubated for a further 6 h. Total proteins from MCF 10A and MCF 12A cells were then analysed for DDX3 protein levels by immunoblot analysis. As shown in Figure 1b (left panel), DDX3 protein levels increased after 3 h of incubation in BPDE in both cell lines, and continued to increase up to 6 h.

Analysis of DDX3 expression in breast epithelial cell lines

To determine whether the expression of DDX3 correlates with breast cancer invasiveness, we performed immunoblot analyses on total protein preparations from a panel of normal immortalized breast cell lines and breast cancer cell lines with varying degree of invasiveness. Figure 1b (right panel) shows that the highly tumorigenic cell lines, Hs578T, MDA-MB-468 and MDA-MB-231 contained the highest levels of DDX3 whereas the weakly tumorigenic cell lines, MCF-7 and SK-BR-3, and the immortalized non-tumorigenic mammary epithelial cells, MCF 10A and MCF 12A, expressed relatively low amounts of DDX3.

In addition, we analysed the DDX3 transcript levels on the same series of cell lines using quantitative real-time PCR (qRT–PCR). Figure 1c indicates that DDX3 mRNA expression increases as the tumorigenicity increases, with the highest levels observed in MDA-MB-231 cells. These results indicate that the mRNA and protein levels of DDX3 are higher in aggressive breast cancer cell lines as compared to the immortalized breast cell lines.

MCF 10A-DDX3 transgenic cells undergo an epithelial-mesenchymal-like transition

In an effort to identify the effects of DDX3 overexpression on cellular phenotype, we generated MCF 10A cells that stably overexpress DDX3. Stable expression of DDX3 generated distinct spindle-shaped cells rather than the normal cuboidal MCF 10A phenotype (Figure 2a). As shown in Figure 2b, immunofluorescence confirmed the overexpression of DDX3 in these transformants. MDA-MB-231 cells were used as a positive control for DDX3 expression. We then analysed the growth properties of these cells using Matrigel assays. As depicted in Figure 2c, the parental MCF 10A

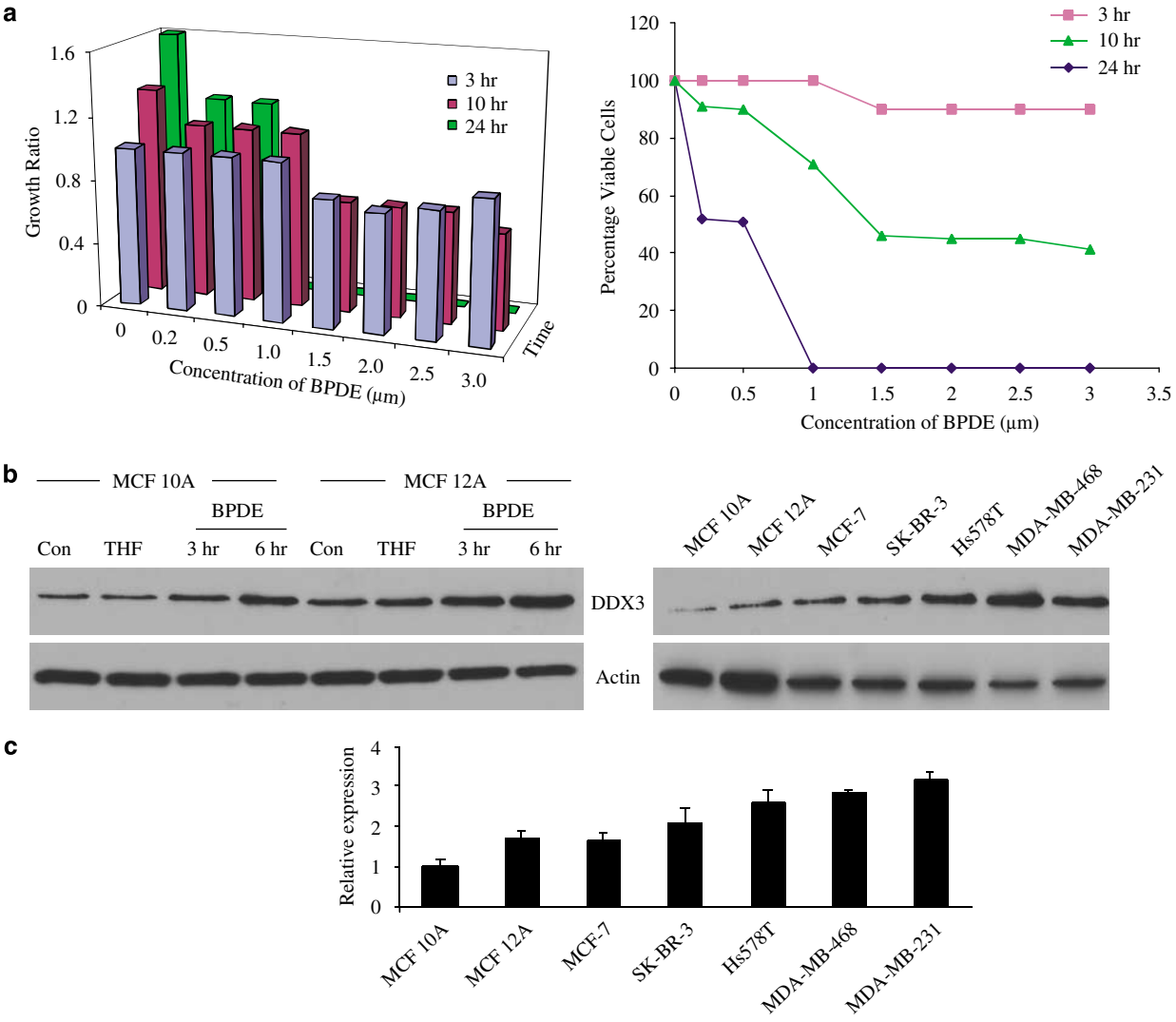

Figure 1 Induction of DDX3 by BPDE in mammary epithelial cells. (**a**) Effect of BPDE on the growth (left) and viability (right) of MCF 10A cells in a time-dependent manner. (**b**) Left: immunoblot analyses of the levels of DDX3, at different incubation time points, in MCF 10A and MCF 12A cells following incubation with 0.5 μM BPDE. Right: immunoblot analyses of the levels of DDX3 protein in a panel of immortalized mammary epithelial cells and breast cancer cell lines. (**c**) Relative DDX3 mRNA expression level quantified by real-time PCR in an identical panel of cell lines as in (**b**) right. BPDE, benzo[a]pyrene diol epoxide; con, control cells; THF, tetrahydrofuran.

cells retained the ability to grow and spread in a contact-dependent manner. On the other hand, MCF 10A-DDX3 cells exhibited a growth pattern in Matrigel that resulted in compact spherical structures, indicative of a loss of contact inhibition growth. Thus, overexpression of DDX3 in MCF 10A cells gave rise to contact-independent growth in Matrigel with the subsequent formation of dense spheroid bodies. The use of Calcein AM staining demonstrated that the dense spheroid bodies contained live cells (data not shown). A protracted incubation (4 weeks) of these plates showed that MCF 10A-DDX3 cells attained the ability to grow as individual cells rather than as colonies, indicative of contact-independent growth.

Anchorage-independent growth is another growth property of aggressive cancer cells. To test if MCF 10A-DDX3 cells can grow independent of attaching to a substratum, soft agar colony-forming assays were performed. As shown in Figure 2d, on average, MCF 10A-DDX3 cells formed 750 colonies per plate compared to only 5 colonies per plate for parental MCF 10A cells. Two independent clones were analysed that exhibited consistent results. Taken together, these results provide strong evidence that overexpression of DDX3 can alter the cellular characteristics of MCF 10A cells to that of an aggressive phenotype.

DDX3 increases motility and invasion in MCF 10A cells

One of the characteristics of epithelial-mesenchymal transition is an increase in cell motility and invasion. To test whether overexpression of DDX3 in MCF 10A cells promotes motility and invasion, cells were grown in boyden chambers in the presence of mitogen. As shown

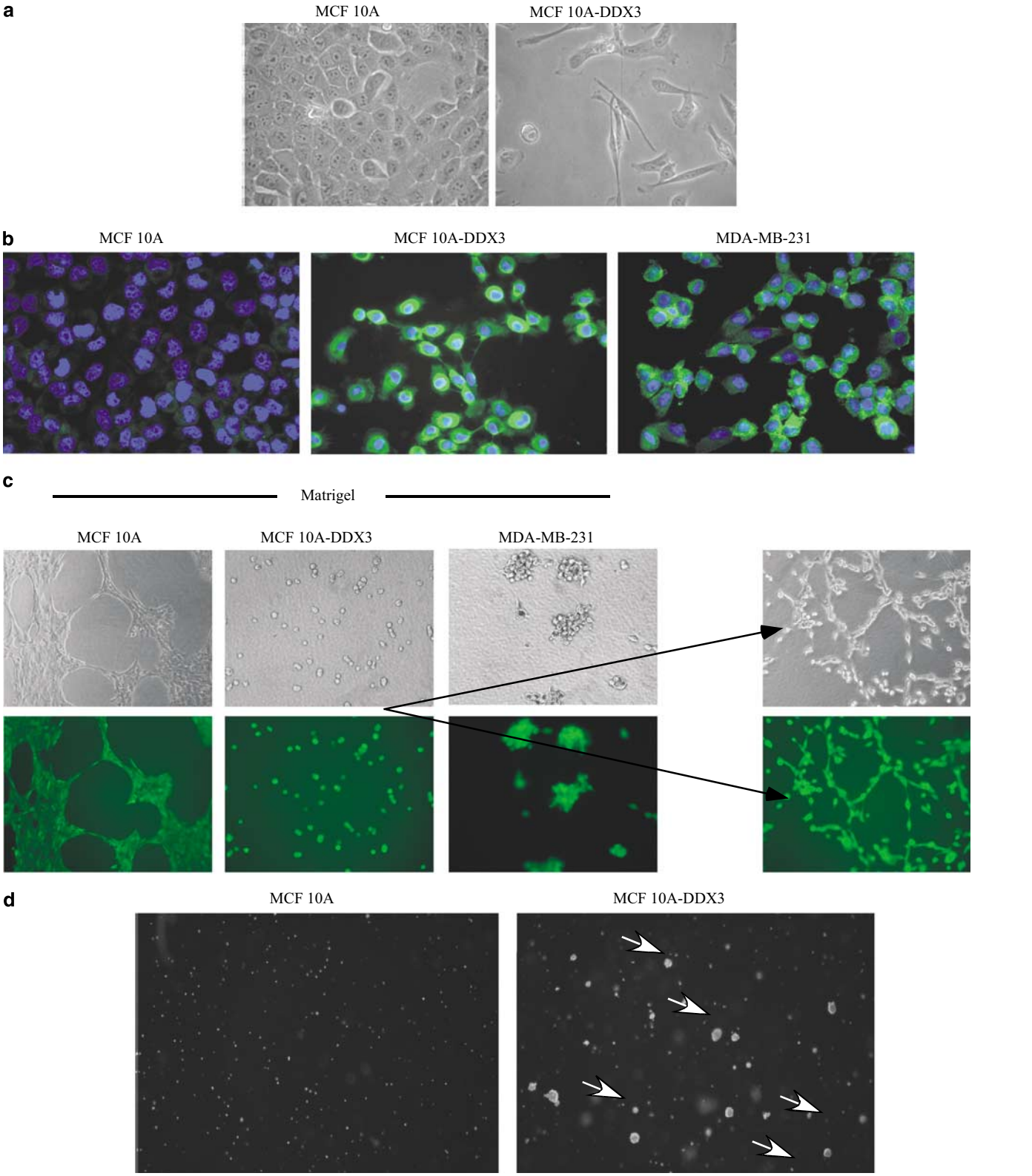

Figure 2 Phenotypic characterization of MCF 10A-DDX3 cells. (**a**) Photomicrographs of MCF 10A-DDX3 cells (spindle-shaped) as compared to the parental MCF 10A cells (cuboidal). (**b**) Immunocytochemistry using anti-DDX3 antibody on MCF 10A, MCF 10A-DDX3 and MDA-MB-231 (positive control) cells. Secondary antibody against anti-DDX3 was labeled with AlexaFluor 488 (green fluorescence). Nuclei were stained with 4,6-diamidino-2-phenylindole (blue fluorescence). (**c**) Growth characteristics of MCF 10A, MCF 10A-DDX3 and MDA-MB-231 on Matrigel. Arrows indicate the morphology of MCF 10A-DDX3 after a 4-week growth period. Calcein AM staining (green) was performed to identify live cells. (**d**) Colony-forming ability of MCF 10A-DDX3 cells on soft agar relative to the parental cell line. Arrows indicate growing colonies.

in Figure 3a, MCF 10A-DDX3 cells exhibited motility that was an order of magnitude greater than the parental MCF 10A cells, that is, 18 versus 1.5% respectively. In addition, 3.5 times more MCF 10A-DDX3 cells invaded and migrated through matrigel than the parental MCF 10A cells: 22 versus 6% respectively. To validate this finding, wound-healing experiments were performed. As demonstrated in Figure 3b, MCF 10A-DDX3 cells were able to migrate into the cleared area within less than 18 h of incubation. On the other hand, MCF 10A cells showed little colonization of the cleared region during this time period. The lower panels of Figure 3b are higher magnification images, which indicate the spindle-shaped MCF 10A-DDX3 cells colonizing the empty space while the cuboidal MCF 10A cells have largely accumulated near the boundary of the cleared area. This result, in combination with the boyden chamber experiments, indicates that DDX3-overexpressing cells are more motile and invasive than MCF 10A cells.

DDX3 alters the localization of β-catenin in breast cells

Following the observation that DDX3 induces an epithelial-mesenchymal-like transition, we performed microarray analysis, which identified E-cadherin as a downstream target gene whose expression was reduced 19-fold in MCF 10A-DDX3 cells. This reduction was verified at the protein level. As shown in Figure 4a, MCF 10A-DDX3 cells expressed little or no E-cadherin protein as compared to MCF 10A cells. As E-cadherin is associated with several cytoplasmic proteins including β-catenin, which directly interacts with E-cadherin, we compared the localization of E-cadherin and β-catenin in MCF 10A and MCF 10A-DDX3 cell lines by immunocytochemistry. As shown in Figure 4a (right panel), in MCF 10A cells, the E-cadherin (red) was predominantly localized at the cell membrane along with the majority of the β-catenin (green) staining. In both cases, this membrane-staining pattern was readily apparent at juxtaposed lateral cell–cell surface boundaries. On the other hand, in MCF 10A-DDX3 cells, there was little or no E-cadherin expression at the cell membrane (Figure 4a, right panel). In this case, β-catenin staining was diffuse with the majority being observed in the cytoplasm and to some extent in the nucleus. Merged images indicate the colocalization of E-cadherin and β-catenin (yellow-green) at the plasma membrane of MCF 10A cells, but not in MCF 10A-DDX3 cells. Similar results were obtained using two independent MCF 10A-DDX3 clones. These experiments indicate that in MCF 10A-DDX3 cells, the loss of E-cadherin at the plasma membrane results in a shift in the subcellular location of β-catenin from the membrane to the cytosol and nucleus.

DDX3 represses E-cadherin promoter-reporter activity

To determine whether DDX3 transcriptionally represses E-cadherin expression, co-transfection experiments were performed in breast cancer cell lines using effector plasmid (DDX3-expressing) along with reporter

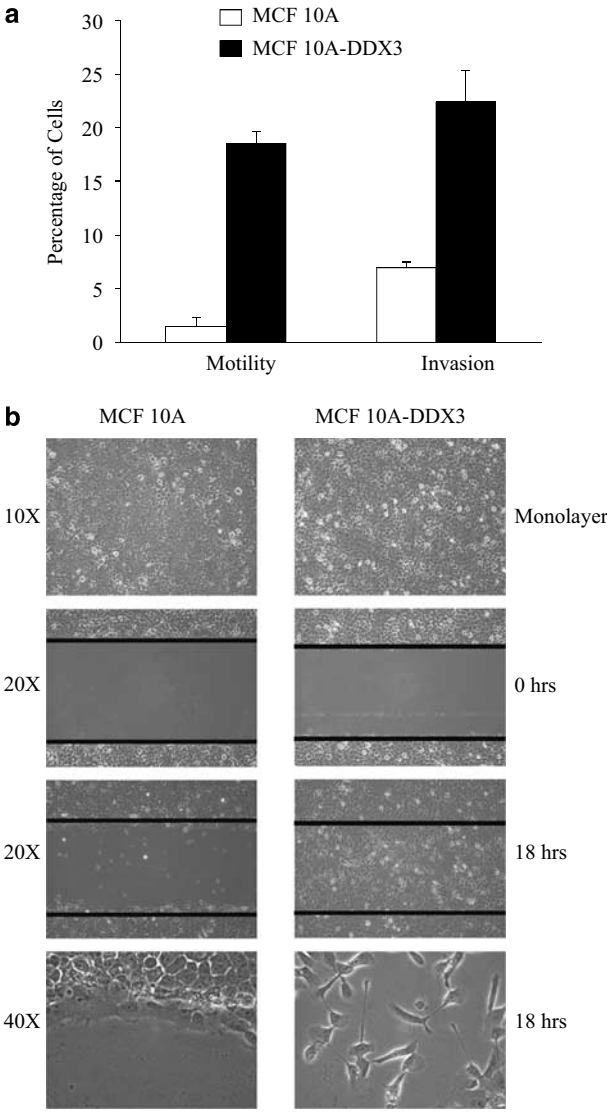

Figure 3 Stable expression of DDX3 in MCF 10A cells increased motility and invasion of MCF 10A cells. (**a**) Bar graph represents motility and invasion of MCF 10A-DDX3 as compared to the parental MCF 10A cells. Results shown are the means (±s.d.) of three independent experiments. (**b**) *In vitro* wound-healing/scratch assay. A clearing, as demarcated by the horizontal black lines, through confluent monolayers of MCF 10A and MCF 10A-DDX3 cells was generated with a sterile pipet tip. Photomicrographs were obtained at the indicated time points with the indicated magnifications. The strikingly different phenotypes of MCF 10A and MCF 10A-DDX3 cells are readily seen at the edge of the 'wound' with ×40 magnification (bottom images).

constructs carrying the luciferase (Luc) gene driven by the E-cadherin promoter sequences of varying length. As shown in Figure 4b (right panel), DDX3 repressed Luc activity of the E1 and E2 construct by 8- and 14–fold, respectively. E3 and E5 constructs showed an average of two- to threefold repression of Luc activity. Thus, in this system, the most active *cis*-element(s) responsible for the direct or indirect regulation of the E-cadherin promoter by DDX3 is positioned between −995 and −677 bp relative to the transcription start site.

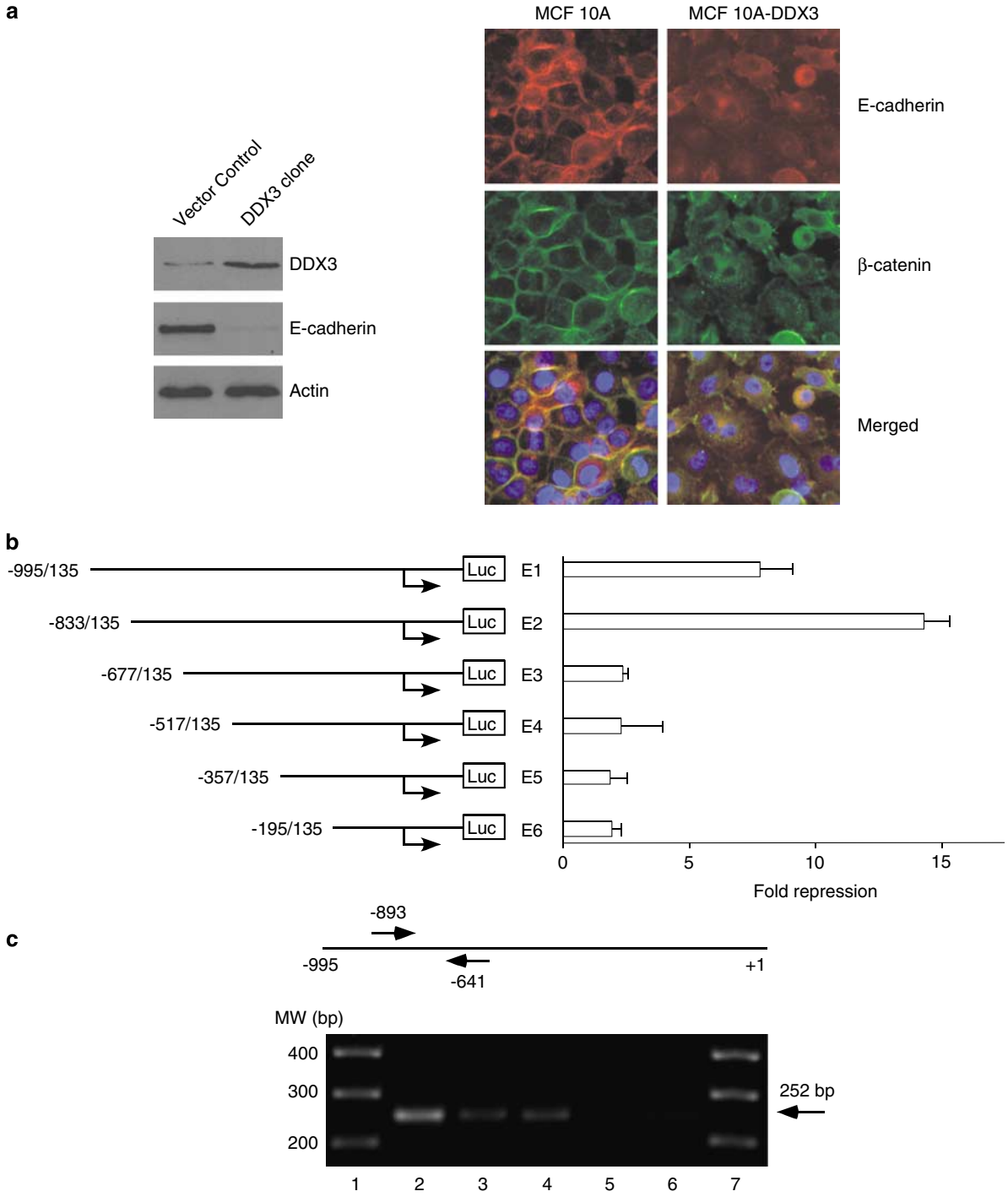

Figure 4 Overexpression of DDX3 represses E-cadherin expression in breast cells. (**a**) Left: immunoblot analyses for E-cadherin and DDX3 levels in MCF 10A and MCF 10A-DDX3 cells. Actin was scored for the loading control. Right: immunocytochemistry for E-cadherin (red) and β-catenin (green) in MCF 10A and MCF 10-DDX3 cells. Colocalization of the two signals is shown as yellow-green in the merged image. (**b**) Luciferase (Luc)-based reporter assay. At the left are schematic representations of the E-cadherin promoter constructs (E1–E6), which ranged from −995 to −195 bp upstream of transcription start site to 135 bases downstream of the transcription start site. The bar graph to the right indicates the fold repression of Luc activity in the presence of DDX3. All experiments were done in replicates and repeated at least three times. (**c**) *In vivo* binding of DDX3 to the E-cadherin in MCF 10A-DDX3 cells was analysed using E-cadherin promoter-specific primers by PCR. Top panel: schematic representation of the E-cadherin promoter. Arrows represent the region amplified by PCR for the chromatin immunoprecipitation experiment. Bottom panel: lanes 1 and 7—molecular weight (MW) marker; lane 2—total input chromatin; lane 3—acetyl histone H3 precipitation; lane 4—DDX3 antibody; lane 5—nonspecific antibody; and lane 6—no antibody precipitation. Identical volumes from the final precipitate were used for PCR (except for the input chromatin, which was diluted 100 ×). PCR was performed with primers (5′-CAACATGGT GAAACCCCGTCTG-3′, and antisense, 5′-GTGAGCCATGAGCCACTGAGCT-3′) spanning the −893 to −641 region of the E-cadherin promoter.

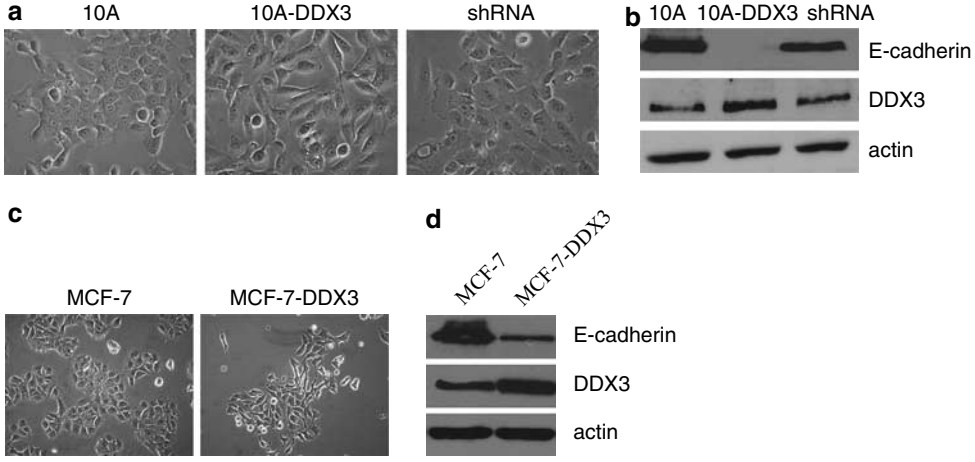

Figure 5 Knockdown of DDX3 by shRNA promotes E-cadherin expression. Stable shRNA clones against DDX3 were generated in MCF 10A-DDX3 cells. (**a**) Morphology of the shRNA clone as compared to the parental MCF 10A-DDX3 cells. (**b**) Immunoblot showing E-cadherin and DDX3 protein levels in the shRNA clone. (**c**) Morphology of MCF-7 cells overexpressing DDX3. (**d**) Protein levels of E-cadherin and DDX3 in the transgenic MCF-7-DDX3 clone. shRNA, short hairpin RNA.

DDX3 binds to the E-cadherin promoter in vivo

To confirm that the downregulation of E-cadherin was due to the binding of DDX3 either directly or indirectly to the promoter region, we performed chromatin immunoprecipitation (ChIP) assays using MCF 10A-DDX3 cells. PCR was designed to amplify the region from −893 to −641 bp of the E-cadherin promoter, as schematically shown in Figure 4c. DNA precipitates from anti-DDX3 antibody incubation were amplified using E-cadherin promoter-specific primers (lane 4; Figure 4c). The same was true in unprocessed chromatin as well as in anti-acetyl-histone precipitations (lanes 2 and 3 respectively; Figure 4c). However, no amplified products were observed when either a nonspecific antibody or no antibody was used (lanes 5 and 6 respectively; Figure 4c). These results indicate that DDX3 binds either directly or as part of a heterogeneous complex to the endogenous E-cadherin promoter.

Downregulation of DDX3 by shRNA promotes E-cadherin expression

To validate the specific regulation of E-cadherin expression by DDX3, short hairpin RNA (shRNA) clones against DDX3 were generated in MCF 10A-DDX3 cells. As shown in Figure 5a, representative clone of shRNA-DDX3 did exhibit variant colony morphology as compared to the parental clone. Analysis of DDX3 and E-cadherin protein levels clearly demonstrates the re-expression of E-cadherin in the shRNA clone (Figure 5b). In addition, overexpression of DDX3 in another breast cancer cell, MCF-7, resulted in the decrease of E-cadherin expression (Figures 5c and d). Taken together, these results are strong supporting evidence that indicates that DDX3 has an important function in the regulation of E-cadherin expression in these cell lines.

Regulation of tumor suppressor molecule p21Waf1/Cip1 by DDX3

Recently, Chao *et al*. (2006) showed that DDX3 could cause growth arrest of liver tumor cells by inducing p21 expression. However, our results indicate that DDX3 promotes anchorage-independent growth with increased motility and invasive properties. This led us to assess the functional role of DDX3 in regulating p21 expression in breast cancer cells. Initially, we performed qRT–PCR to identify the p21 mRNA expression levels in MCF 10A and two independent MCF 10A-DDX3 clones. As shown in Figure 6a (left panel), levels of p21 mRNA were reduced in the MCF 10A-DDX3 cells compared to the MCF 10A cells. Next, we performed qRT–PCR on a panel of breast cancer cell lines to correlate the expression levels of DDX3 with p21 among breast cell lines. As shown in Figure 6b, increased expression of DDX3 did not upregulate the expression of p21 in most aggressive breast cancer cell lines such as MDA-MB-231 and MDA-MB-468 as compared to MCF 10A and MCF 12A cell lines. However, an increase in p21 levels was observed in MCF-7, SK-BR-3 and Hs578T breast cancer cell lines. This is probably due to the genetic heterogeneity of the derived cell lines. Also, the stability of the mRNA and the post-transcriptional regulation may contribute to the synthesis of p21 protein levels.

Next, we performed p21 promoter-reporter assays in MCF-7 cells in the presence and absence of exogenous DDX3. As shown in Figure 6c, the use of either 2.3 or 0.16 kb p21 promoter-reporter construct did not show any increase in Luc activity in the presence of DDX3 (Zeng *et al*., 1997). Thus, these results indicate that DDX3 could have divergent roles in different tumor types as aggressive breast cancer cells have relatively high levels of DDX3 and low levels of p21, which is the opposite of that reported for liver cancer.

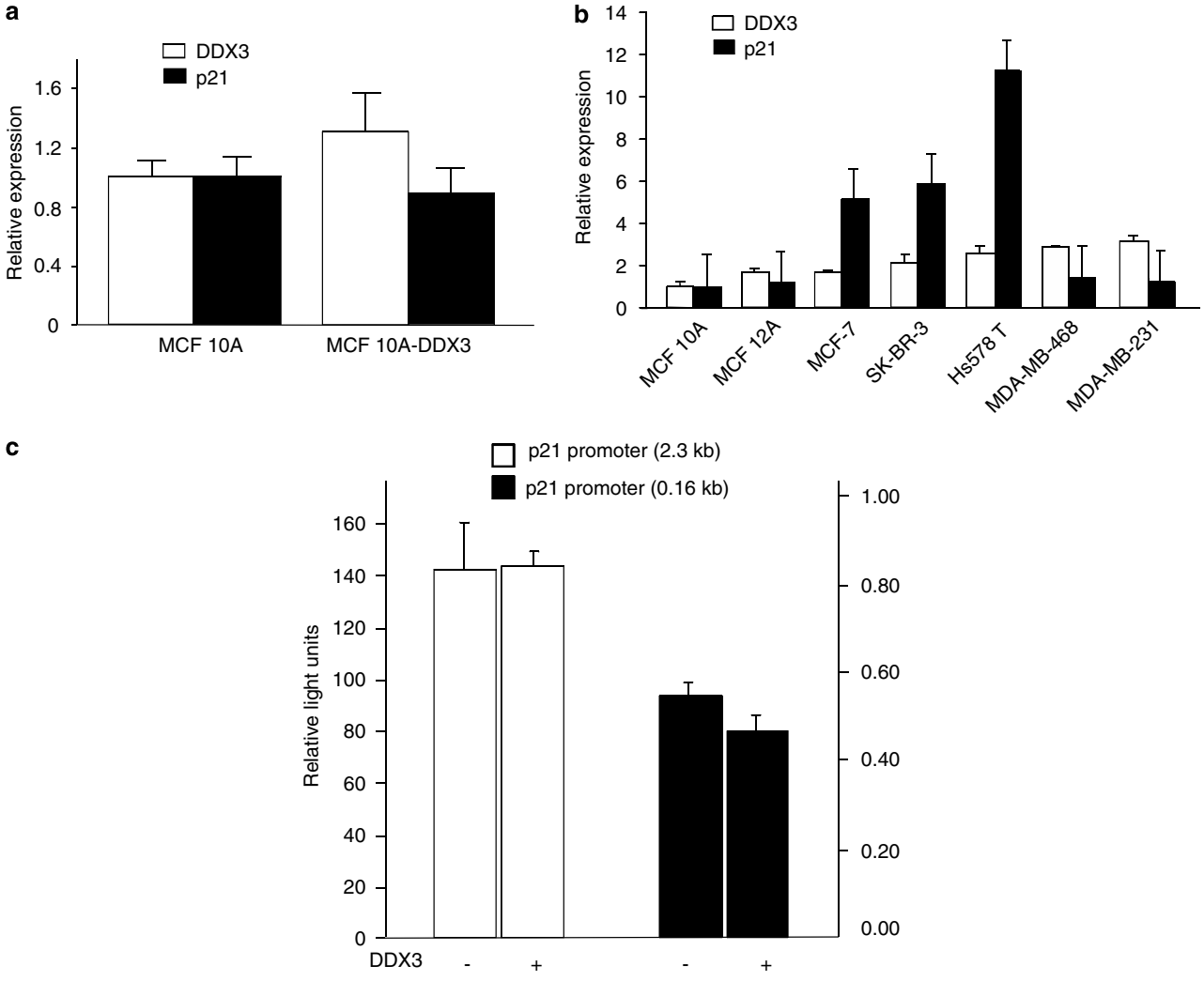

Figure 6 Lack of correlation between DDX3 and p21 levels in breast cells. (**a**) Histogram showing relative fold expression ($2^{-(\Delta\Delta Ct)}$) values of p21 mRNA in MCF 10A and MCF 10A-DDX3 cell lines. The p21 expression levels were downregulated in MCF 10A-DDX3 relative to MCF 10A cell line. (**b**) Quantitative real-time PCR analyses of DDX3 and p21 mRNA levels ($2^{-(\Delta\Delta Ct)}$) in a panel of immortalized mammary epithelial cells and breast cancer cell lines. (**c**) p21 promoter-reporter assays with DDX3 as the effector molecule. The luciferase activities were analysed from the cell lysates transfected with DDX3 and the p21 promoter-reporter constructs. Reporter activity was measured as relative light units. White columns represent 2.3 Kb and black columns represent 0.16 Kb of the p21 promoter region, respectively.

Discussion

Exposure to tobacco smoke is relatively common among the US population as an estimated 43% reside with at least one smoker (Pirkle *et al*., 1996). However, there is conflicting evidence with respect to tobacco smoke as a causative agent in breast cancer biogenesis (Reynolds *et al*., 2004; Bonner *et al*., 2005). To address these questions, we initiated studies to decipher the effects of tobacco smoke constituents on the growth and proliferation of breast cells. In our model, non-tumorigenic immortalized breast epithelial cells (MCF 10A) were exposed to increasing concentrations of the highly reactive metabolite of B[a]P, BPDE, a potent carcinogen found in tobacco smoke (Reynolds *et al*., 2004). Exposure of MCF 10A cells to BPDE resulted in detectable changes in the growth and viability of MCF 10A cells. Under these conditions, BPDE induced a number of genes belonging to DNA damage/repair and cell-stress pathways, including the DEAD box RNA helicase, DDX3.

To characterize the function(s) of DDX3 in breast epithelial cells, we generated MCF 10A-DDX3 cells, which constitutively overexpress DDX3. MCF 10A-DDX3 cells exhibited a fibroblastic phenotype that is strikingly different from the normal epithelial-like cuboidal-shaped MCF 10A cells. Similar morphological changes are observed during an epithelial-to-mesenchymal transition, which is a hallmark of cancer progression in several types of cancers (Mironchik *et al*., 2005; Whitbread *et al*., 2006; Jung *et al*., 2007). Evidence supportive of the concept that MCF 10A-DDX3 cells are likely an aggressive cell line was obtained from experiments showing anchorage-independent growth on

soft agar. Growth on soft agar is indicative of loss of contact growth inhibition as well as a transformed phenotype (Burdick *et al*., 2006). The invasive potential of MCF 10A-DDX3 cells was tested in a Matrigel-based invasion assay. The tubular networks formed by MCF 10A-DDX3 cells in Matrigel were indistinguishable from structures formed by the established aggressive breast cancer cell line MDA-MB-231. This type of invasion involves degradation of the extracellular matrix by proteolytic enzymes such as matrix metalloproteases (Yokoyama *et al*., 2003). We have found that matrix metalloprotease-2 mRNA levels in MCF 10A-DDX3 cells were increased 3.6-fold relative to MCF 10A cells (data not shown). Increased levels of enzymes such as matrix metalloprotease-2 probably contribute to the increased rate of invasion of MCF 10A-DDX3 cells through Matrigel. Similarly, in motility assays, MCF 10A-DDX3 cells exhibited higher motility as compared to MCF 10A cells. The role of DDX3 in promoting aggressive phenotype was observed in two independent MCF-10A-DDX3 clones, indicating a consistent oncogenic function. The data summarized here provide strong evidence that MCF 10A-DDX3 cells gained invasive capability, which is indicative of a transformation to an aggressive phenotype.

An important characteristic of normal epithelial cells is the adhesion between cells, which is mediated in part by adherens junctions. E-cadherin is an essential component of adherens junctions and is constitutively expressed in normal epithelial cells (Takeichi, 1990). Loss of its expression results in increased migration and proliferation of cells, leading to invasion and has been correlated to poor prognosis in the clinic (Shimoyama *et al*., 1989; Margulis *et al*., 2005). Thus, our finding that E-cadherin was downregulated in MCF 10A-DDX3 cells relative to MCF 10A cells was an important finding that warranted further investigation. In an attempt to decipher the mechanism by which DDX3 downregulates E-cadherin expression, we performed Luc-based promoter-reporter assays, which showed that DDX3 might modulate E-cadherin expression at the transcriptional level. The transcriptional role of DDX3 is similar to that in other reports that have indicated that DEXD/DEAH box helicases can participate in the transcriptional regulation of estrogen receptor and p16INK4 (Myohanen and Baylin, 2001; Rajendran *et al*., 2003). In addition, immunocytochemistry experiments indicate that a consequence of the DDX3-mediated suppression of E-cadherin is the altered subcellular localization of β-catenin from the plasma membrane to the cytosol and nucleus.

Recently, DDX3 has been shown to induce the transcriptional activity of the $p21^{waf1/cip1}$ gene via interaction with Sp1 at the promoter region and reduce cell growth and proliferation in hepatocarcinoma (Chao *et al*., 2006). However, based on our data using immortalized breast cell lines and breast cancer cells, we show that DDX3 expression correlates with aggressive phenotype and does not attenuate cell growth and proliferation. It is possible that the regulatory mechanisms of DDX3 in varied cell types are different depending upon the presence of appropriate cofactors and/or signaling pathways (Marchetti *et al*., 1996; Myohanen and Baylin, 2001). Also, truncating mutations of DDX3 may exist that can alter its functions in different cell types. However, based on our immunoblot data, using breast cancer cell lines, we were unable to detect any truncated version of DDX3. In addition, there was no overamplification of DDX3 (data not shown) within our panel of breast cancer cell lines (MCF 10A, MCF 10A-DDX3, MCF 12A, MCF-7, Hs578T, SK-BR-3, MDA-MB-468 and MDA-MB-231), indicating that gene amplification is probably not one of the mechanisms by which overexpression of DDX3 is accomplished. Alternative mechanisms such as increased mRNA stability or translation and decreased protein turn over could be involved in regulating the levels of DDX3.

Overall, our results indicate that the activation of DDX3 by BPDE can induce neoplastic transformation in breast cells with concomitant increase in motility and invasion. Also, overexpression of DDX3 can induce anchorage-independent growth, epithelial-mesenchymal-like transition and downregulate E-cadherin expression. Finally, the broader implication of this research is that potent carcinogens found in tobacco smoke can initiate and promote breast cancer progression and one such mechanism is through the activation of DDX3, a member of DEAD box helicases.

Materials and methods

Cell culture and BPDE exposure

MCF 10A cells were treated with 0.2, 0.5, 1, 1.5, 2, 2.5 or 3 μM of BPDE for 3, 10 and 24 h. Following treatment, the cells were washed, trypsinized and collected for cell viability analysis using the trypan blue exclusion assay. In a separate experiment, total RNA and proteins were isolated following BPDE induction.

Expression profile of DDX3 in breast cell lines

Quantitative real-time PCR and immunoblotting were carried out to determine the expression level of DDX3 in a panel of immortalized normal breast cell lines and breast cancer cell lines. Total RNA was isolated from MCF 10A, MCF 12A, Hs578T, MCF-7, SK-BR-3, MDA-MB-468 and MDA-MB-231 cell lines using TRIzol (Invitrogen, Carlsbad, CA, USA) reagent according to the manufacturer's protocol. qRT–PCR was performed with DDX3 sense 5′-GGAGGAAGTACAGC CAGCAAAG-3′ and antisense 5′-CTGCCAATGCCATCG TAATCACTC-3′ primers. DDX3 protein levels were detected by immunoblots using monoclonal anti-DDX3 antibody (in-house generated). Briefly, a bacterially expressed glutathione *S*-transferase-tagged full-length DDX3 fusion protein was used as antigen to generate the monoclonal antibody, which specifically recognizes the N-terminal 142 aa of DDX3.

Colony-formation assays

MCF 10A or MCF 10A-DDX3 cells (1×10^4) were suspended in 2 ml of 0.4% (wt/vol) Sea Plaque Agarose (FMC BioProducts, Rockland, ME, USA) containing Dulbecco's modified Eagle's medium supplemented with 10% fetal bovine serum and overlaid onto a 1% (wt/vol) Sea Plaque Agarose

solution in 35-mm plates. Following incubation for 2–3 weeks, the colonies were stained with trypan blue and counted. All experiments were performed in triplicate.

Wound-healing assay
Monolayers of MCF 10A and MCF 10A-DDX3 cells grown in 10 cm dishes were cleared along a diameter of the plate, with a sterile pipette tip. Cell migration was measured and photographed (using a Nikon TS100 microscope) from the wound/scratch edge every 9 h. All experiments were performed in triplicate.

Invasion and motility assays
Matrigel (100 μl; 7–8 mg ml^{-1}) in serum-free medium was added to each well of a Transwell Corning Costar plate (Costar, Acton, MA, USA) and dried overnight in a tissue culture hood. The following day, 2.5×10^4 cells in serum-free medium were pipetted onto the Matrigel and complete medium was added to the bottom trough. Following incubation, the transmembrane filter was stained with crystal violet and the number of cells counted. Motility assays were performed similar to the invasion assay, except that Matrigel was omitted. All experiments were performed in triplicate.

Reporter assays
Activity of the reporter gene in pGL2-Basic-E-cadherin promoter deletion constructs was assayed using the Luciferase Reporter Assay kit (Promega, Madison, WI, USA) according to the manufacturer's instructions. Reporter constructs (250 ng) were co-transfected into MCF-7 breast cancer cells (5×10^4 cells) with 750 ng of pCDNA-DDX3 (effector plasmid) plus 50 ng of GFP plasmid using Trans IT-LT (Mirus, Madison, WI, USA) transfection reagent and the cells were incubated for 24 and 48 h. Following incubation, cell lysates were harvested and the luciferase activity measured (Luminometer-Berthhold Detection System, Oak Ridge, TN, USA). All experiments were performed in triplicate.

Chromatin immunoprecipitation assay
Chromatin immunoprecipitation was carried out following established protocols using the MCF 10A-DDX3 cell line as previously reported (Duriseti *et al*., 2006). Chromatin–protein complexes were immunoprecipitated using monoclonal anti-DDX3 or anti-acetyl-histone antibodies. Anti-actin antibody and samples prepared without antibodies served as negative controls.

Immunofluorescence
MCF 10A and MCF 10A-DDX3 (2×10^4) were plated onto four-well chamber glass slides, fixed, permeabilized, washed and incubated for 1 h at room temperature with mouse anti-E-cadherin plus rabbit anti-β-catenin antibodies (1:1000, Transduction Laboratories, Lexington, KY, USA) followed by secondary fluorescent antibodies. Nuclei were counterstained with 4,6-diamidino-2-phenylindole and mounted with DPX (Fluka Biochemicals, Milwaukee, WI, USA), dried (4 °C, overnight) and examined using a Nikon Eclipse 80i fluorescence microscope. Images were recorded and processed with Image ProPlus 5 (Media Cybernetics) software.

Knockdown of DDX3 by shRNA
The shRNA-expressing vector was generated by cloning the annealed sense (5′-GATCCCCGCAAATTTGAACGTGGTG GTTCAAGAGACCACCACGTTCAAATTTGCTTTTTC-3′) and antisense (5′-TCGAGAAAAAGCAAATTTGAACGTG GTGGTCTCTTGAACCACCACGTTCAAATTTGCGGG-3′) strands into pSUPER vector. Stable shRNA clones against DDX3 were generated in MCF 10A-DDX3 cells using Trans IT-LT (Mirus) transfection reagent. Three clones of the shRNA and the MCF-7-DDX3 clones were analysed.

Abbreviations

BPDE, benzo[a]pyrene diol epoxide; ChIP, chromatin immunoprecipitation; qRT–PCR, quantitative real-time PCR.

Acknowledgements

This work was supported by a grant from the Fight Attendant Medical Research Institute (FAMRI) to Venu Raman. p21 promoter-reporter constructs were kindly provided by Dr Wafik El-Deiry (University of Pennsylvania).

References

Abdelhaleem M. (2005). RNA helicases: regulators of differentiation. *Clin Biochem* **38**: 499–503.

Boffetta P, Hashibe M, La Vecchia C, Zatonski W, Rehm J. (2006). The burden of cancer attributable to alcohol drinking. *Int J Cancer* **119**: 884–887.

Bonner MR, Nie J, Han D, Vena JE, Rogerson P, Muti P *et al*. (2005). Secondhand smoke exposure in early life and the risk of breast cancer among never smokers (United States). *Cancer Causes Control* **16**: 683–689.

Burdick AD, Ivnitski-Steele ID, Lauer FT, Burchiel SW. (2006). PYK2 mediates anti-apoptotic AKT signaling in response to benzo[a]pyrene diol epoxide in mammary epithelial cells. *Carcinogenesis* **27**: 2331–2340.

Caruso JA, Reiners Jr JJ, Emond J, Shultz T, Tainsky MA, Alaoui-Jamali M *et al*. (2001). Genetic alteration of chromosome 8 is a common feature of human mammary epithelial cell lines transformed *in vitro* with benzo[a]pyrene. *Mutat Res* **473**: 85–99.

Chang PC, Chi CW, Chau GY, Li FY, Tsai YH, Wu JC *et al*. (2006). DDX3, a DEAD box RNA helicase, is deregulated in hepatitis virus-associated hepatocellular carcinoma and is involved in cell growth control. *Oncogene* **25**: 1991–2003.

Chao CH, Chen CM, Cheng PL, Shih JW, Tsou AP, Lee YH. (2006). DDX3, a DEAD box RNA helicase with tumor growth-suppressive property and transcriptional regulation activity of the p21waf1/cip1 promoter, is a candidate tumor suppressor. *Cancer Res* **66**: 6579–6588.

Cordin O, Banroques J, Tanner NK, Linder P. (2006). The DEAD-box protein family of RNA helicases. *Gene* **367**: 17–37.

Duriseti S, Winnard Jr PT, Mironchik Y, Vesuna F, Raman A, Raman V. (2006). HOXA5 regulates hMLH1 expression in breast cancer cells. *Neoplasia* **8**: 250–258.

Huang JS, Chao CC, Su TL, Yeh SH, Chen DS, Chen CT *et al*. (2004). Diverse cellular transformation capability of overexpressed genes in human hepatocellular carcinoma. *Biochem Biophys Res Commun* **315**: 950–958.

Jeffy BD, Chirnomas RB, Chen EJ, Gudas JM, Romagnolo DF. (2002). Activation of the aromatic hydrocarbon receptor pathway is not sufficient for transcriptional repression of BRCA-1: requirements for metabolism of benzo[a]pyrene to 7r, 8t-dihydroxy-9t, 10-epoxy-7, 8, 9, 10-tetrahydrobenzo[a]pyrene. *Cancer Res* **62**: 113–121.

Jung JW, Hwang SY, Hwang JS, Oh ES, Park S, Han IO. (2007). Ionising radiation induces changes associated with

epithelial-mesenchymal transdifferentiation and increased cell motility of A549 lung epithelial cells. *Eur J Cancer* **43**: 1214–1224.

Krolewski B, Little JB, Reynolds RJ. (1988). Effect of duration of exposure to benzo(a)pyrene diol-epoxide on neoplastic transformation, mutagenesis, cytotoxicity, and total covalent binding to DNA of rodent cells. *Teratog Carcinog Mutagen* **8**: 127–136.

Linder P. (2006). Dead-box proteins: a family affair–active and passive players in RNP-remodeling. *Nucleic Acids Res* **34**: 4168–4180.

Marchetti A, Doglioni C, Barbareschi M, Buttitta F, Pellegrini S, Bertacca G *et al*. (1996). p21 RNA and protein expression in non-small cell lung carcinomas: evidence of p53-independent expression and association with tumoral differentiation. *Oncogene* **12**: 1319–1324.

Margulis A, Zhang W, Alt-Holland A, Crawford HC, Fusenig NE, Garlick JA. (2005). E-cadherin suppression accelerates squamous cell carcinoma progression in three-dimensional, human tissue constructs. *Cancer Res* **65**: 1783–1791.

Mei J, Hu H, McEntee M, Plummer III H, Song P, Wang HC. (2003). Transformation of non-cancerous human breast epithelial cell line MCF10A by the tobacco-specific carcinogen NNK. *Breast Cancer Res Treat* **79**: 95–105.

Mironchik Y, Winnard Jr PT, Vesuna F, Kato Y, Wildes F, Pathak AP *et al*. (2005). Twist overexpression induces *in vivo* angiogenesis and correlates with chromosomal instability in breast cancer. *Cancer Res* **65**: 10801–10809.

Myohanen S, Baylin SB. (2001). Sequence-specific DNA binding activity of RNA helicase A to the p16INK4a promoter. *J Biol Chem* **276**: 1634–1642.

Norsa'adah B, Rusli BN, Imran AK, Naing I, Winn T. (2005). Risk factors of breast cancer in women in Kelantan, Malaysia. *Singapore Med J* **46**: 698–705.

Owsianka AM, Patel AH. (1999). Hepatitis C virus core protein interacts with a human DEAD box protein DDX3. *Virology* **257**: 330–340.

Parkin DM, Muir CS. (1992). Cancer incidence in five continents. Comparability and quality of data. *IARC Sci Publ*, 45–173.

Pfeifer GP, Denissenko MF, Olivier M, Tretyakova N, Hecht SS, Hainaut P. (2002). Tobacco smoke carcinogens, DNA damage and p53 mutations in smoking-associated cancers. *Oncogene* **21**: 7435–7451.

Phillips PH, Linet MS, Harris EL. (1991). Assessment of family history information in case–control cancer studies. *Am J Epidemiol* **133**: 757–765.

Pirkle JL, Flegal KM, Bernert JT, Brody DJ, Etzel RA, Maurer KR. (1996). Exposure of the US population to environmental tobacco smoke: the Third National Health and Nutrition Examination Survey, 1988–1991. *JAMA* **275**: 1233–1240.

Rajendran RR, Nye AC, Frasor J, Balsara RD, Martini PG, Katzenellenbogen BS. (2003). Regulation of nuclear receptor transcriptional activity by a novel DEAD box RNA helicase (DP97). *J Biol Chem* **278**: 4628–4638.

Reynolds P, Hurley S, Goldberg DE, Anton-Culver H, Bernstein L, Deapen D *et al*. (2004). Active smoking, household passive smoking, and breast cancer: evidence from the California Teachers Study. *J Natl Cancer Inst* **96**: 29–37.

Sasco AJ. (2001). Epidemiology of breast cancer: an environmental disease? *APMIS* **109**: 321–332.

Sekiguchi T, Kurihara Y, Fukumura J. (2007). Phosphorylation of threonine 204 of DEAD-box RNA helicase DDX3 by cyclin B/cdc2 *in vitro*. *Biochem Biophys Res Commun* **356**: 668–673.

Shimoyama Y, Hirohashi S, Hirano S, Noguchi M, Shimosato Y, Takeichi M *et al*. (1989). Cadherin cell-adhesion molecules in human epithelial tissues and carcinomas. *Cancer Res* **49**: 2128–2133.

Takeichi M. (1990). Cadherins: a molecular family important in selective cell–cell adhesion. *Annu Rev Biochem* **59**: 237–252.

Toretsky JA, Erkizan V, Levenson A, Abaan OD, Parvin JD, Cripe TP *et al*. (2006). Oncoprotein EWS-FLI1 activity is enhanced by RNA helicase A. *Cancer Res* **66**: 5574–5581.

Wang A, Gu J, Judson-Kremer K, Powell KL, Mistry H, Simhambhatla P *et al*. (2003). Response of human mammary epithelial cells to DNA damage induced by BPDE: involvement of novel regulatory pathways. *Carcinogenesis* **24**: 225–234.

Whitbread AK, Veveris-Lowe TL, Lawrence MG, Nicol DL, Clements JA. (2006). The role of kallikrein-related peptidases in prostate cancer: potential involvement in an epithelial to mesenchymal transition. *Biol Chem* **387**: 707–714.

Yager JD, Davidson NE. (2006). Estrogen carcinogenesis in breast cancer. *N Engl J Med* **354**: 270–282.

Yang D, Louden C, Reinhold DS, Kohler SK, Maher VM, McCormick JJ. (1992). Malignant transformation of human fibroblast cell strain MSU-1.1 by (+-)-7 beta, 8 alpha-dihydroxy-9 alpha, 10 alpha-epoxy-7, 8, 9, 10-tetrahydrobenzo [a]pyrene. *Proc Natl Acad Sci USA* **89**: 2237–2241.

Yang L, Lin C, Liu ZR. (2005). Phosphorylations of DEAD box p68 RNA helicase are associated with cancer development and cell proliferation. *Mol Cancer Res* **3**: 355–363.

Yang L, Lin C, Liu ZR. (2006). P68 RNA helicase mediates PDGF-induced epithelial mesenchymal transition by displacing Axin from beta-catenin. *Cell* **127**: 139–155.

Yang L, Lin C, Zhao S, Wang H, Liu ZR. (2007). Phosphorylation of p68 RNA helicase plays a role in platelet-derived growth factor-induced cell proliferation by up-regulating cyclin D1 and c-Myc expression. *J Biol Chem* **282**: 16811–16819.

Yokoyama K, Kamata N, Fujimoto R, Tsutsumi S, Tomonari M, Taki M *et al*. (2003). Increased invasion and matrix metalloproteinase-2 expression by Snail-induced mesenchymal transition in squamous cell carcinomas. *Int J Oncol* **22**: 891–898.

Zeng YX, Somasundaram K, El-Deiry WS. (1997). AP2 inhibits cancer cell growth and activates p21WAF1/CIP1 expression. *Nat Genet* **15**: 78–82.